Berry Phase, Atom Interferometry, and Observation of the Gravitational Aharonov-Bohm Effect

Huan Q. Bui*
Department of Physics, Massachusetts Institute of Technology

(Dated: May 4, 2022)

Blah

Keywords: Berry phase, Aharonov-Bohm effect, Atom interferometry

I. INTRODUCTION

Section II... outlines some theory. While these topics well-known and are standard subjects of many quantum mechanics textbooks, the author feels compelled to present a short summary to have the essentials at our fingertips.

Section III... presents the experimental observation of the gravitational Aharonov-Bohm effect. The theory and results are addressed. A proposal is reviewed and a recently published work is described. However, the main focus is the experimental technique: atom interferometry.

The author wants this paper to be pedagogical. While some recent observations are discussed, the paper is meant to be an exposition on the theory behind the Berry phase and some underlying principles of atom interferometry.

II. BERRY PHASE

Consider $\mathcal{H}(\boldsymbol{R}(t))$, a time-dependent Hamiltonian parameterized by a family of variables $\boldsymbol{R}(t)$. Let $|\psi(0)\rangle = |n(\boldsymbol{R}(0))\rangle$ where $|n(\boldsymbol{R}(0))\rangle$ is the n^{th} eigenstate of $\mathcal{H}(\boldsymbol{R}(0))$. By the adiabatic theorem, $|\psi(t)\rangle$ is $|n(\boldsymbol{R}(t))\rangle$, the n^{th} instantaneous eigenstate of $\mathcal{H}(t)$, up to a phase factor, i.e.,

$$|\psi(t)\rangle = e^{-\frac{i}{\hbar}\int_0^t E_n(\boldsymbol{R}(t'))\,dt'} \exp(i\gamma_n(t))\,|n(\boldsymbol{R}(t))\rangle\,,$$

where $\gamma_n(t)$ is called the *Berry phase*. Since $|\psi(t)\rangle$ solves the Schrödinger equation $\mathcal{H}(\boldsymbol{R}(t))\,|\psi(t)\rangle = i\hbar(d/dt)\,|\psi(t)\rangle$, we have

$$\dot{\gamma}_n(t) = i\,\langle n(\boldsymbol{R}(t))|\,\nabla_{\boldsymbol{R}}\,|n(\boldsymbol{R}(t))\rangle\cdot\dot{\boldsymbol{R}}(t).$$

In particular, at some final time t_f,

$$\gamma_n(t_f) = \int_{\boldsymbol{R}_i}^{\boldsymbol{R}_f} i\,\langle n(\boldsymbol{R})|\,\nabla_{\boldsymbol{R}}\,|n(\boldsymbol{R})\rangle\cdot d\boldsymbol{R}, \tag{1}$$

which depends only on the path in parameter space over which the evolution takes place. Define the *Berry connection*,

$$\boldsymbol{A}_n(\boldsymbol{R}) = i\,\langle n(\boldsymbol{R})|\,\nabla_{\boldsymbol{R}}\,|n(\boldsymbol{R})\rangle$$

and consider gauge transformation in parameter phase of instantaneous eigenstates $|n(\boldsymbol{R})\rangle \to |\widetilde{n}(\boldsymbol{R})\rangle = e^{-i\beta(\boldsymbol{R})}\,|n(\boldsymbol{R})\rangle$. The Berry connection transforms like the electromagnetic vector potential:

$$\boldsymbol{A}_n(\boldsymbol{R}) \to \widetilde{\boldsymbol{A}_n}(\boldsymbol{R}) = \boldsymbol{A}_n(\boldsymbol{R}) + \nabla_{\boldsymbol{R}}\beta(\boldsymbol{R}).$$

and therefore is also known as the Berry potential. Meanwhile the Berry phase transforms as

$$\widetilde{\gamma_n}(\boldsymbol{R}) = \int_{\boldsymbol{R}_i}^{\boldsymbol{R}_f} \widetilde{A_n}(\boldsymbol{R})\cdot d\boldsymbol{R} = \gamma_n(\boldsymbol{R}_f) + \beta(\boldsymbol{R}_f) - \beta(\boldsymbol{R}_i)$$

which is gauge-invariant exactly when the Hamiltonian evolution is cyclical in parameter space, i.e., $\boldsymbol{R}(t_f) = \boldsymbol{R}(0)$. A remarkable consequence of cyclic evolutions is that the Berry phase is well-defined and is measurable by means of interferometry.

The Berry phase is topological in the sense that it depends on the topology of the parameter space containing the path C along which the system evolves. Consider a closed path C in a parameter space $\mathfrak{R}$. If $\mathfrak{R}$ is one-dimensional, the Berry phase vanishes. In the case that $\mathfrak{R}$ is three-dimensional, Stokes' theorem states that

$$\begin{aligned}\gamma_n(C) &= \oint_C \boldsymbol{A}_n(\boldsymbol{R})\cdot d\boldsymbol{R} \\ &= \iint_S [\nabla_{\boldsymbol{R}}\times\boldsymbol{A}_n(\boldsymbol{R})]\cdot d\vec{S} \equiv \iint_S \boldsymbol{D}_n\cdot d\vec{S}\end{aligned}$$

where S is the surface with boundary C and $\boldsymbol{D}_n \equiv \nabla_{\boldsymbol{R}}\times\boldsymbol{A}(\boldsymbol{R})$ is the *Berry curvature*. We immediately see that if we think of the Berry connection as the electromagnetic vector potential, then the Berry curvature plays the role of the associated magnetic field, which is gauge-invariant. Say something about topological behavior etc and how the notions are separate and Berry phase in topological matter is beyond the scope of the paper.

A. Example: Spin-1/2 in a magnetic field

The Hamiltonian for a spin-1/2 in a magnetic field has the form

$$\mathcal{H}(\boldsymbol{B}) = \boldsymbol{B}\cdot\boldsymbol{\sigma} = r\begin{pmatrix}\cos\theta & \sin\theta e^{-i\phi}\\ \sin\theta e^{i\phi} & -\cos\theta\end{pmatrix}.$$

* huanbui@mit.edu

The eigenvalues are $\pm r$, with associated eigenvectors

$$|+\rangle = \begin{pmatrix} \cos(\theta/2) \\ e^{i\phi}\sin(\theta/2) \end{pmatrix}, \quad |-\rangle = \begin{pmatrix} \cos(\theta/2) \\ -e^{i\phi}\sin(\theta/2) \end{pmatrix}.$$

We require that $r \neq 0$ for the adiabatic theorem to hold. The components of the Berry connection for $|+\rangle$ are readily calculated:

$$\begin{aligned} A_r &= i\langle +|\,\partial_r\,|+\rangle = 0 \\ A_\theta &= i\langle +|\,\partial_\theta\,|+\rangle = 0 \\ A_\phi &= i\langle +|\,\partial_\phi\,|+\rangle = \frac{\cos\theta - 1}{2}. \end{aligned}$$

Here, $\boldsymbol{A}(\boldsymbol{B})$ is actually not defined on the negative z-axis. Consider a closed, piece-wise smooth path C enclosing a surface S such that no point of S lies on the negative z-axis. The Berry phase is

$$\gamma[C] = \oint_C \boldsymbol{A}(\boldsymbol{B})\cdot d\boldsymbol{B} = \iint_S \nabla\times\boldsymbol{A}(\boldsymbol{B})\,d\boldsymbol{S} = -\frac{\Omega}{2}$$

where Ω is nothing but the solid angle enclosed by S. If we had chosen the z-axis to lie in the opposite direction, then the solid angle would have been $|\Omega'| = 4\pi - |\Omega|$. While this appears problematic, $\exp(i\gamma[C])$ is the same in both cases, and the Berry phase is still well-defined.

B. Aharonov-Bohm Effect

The Aharonov-Bohm effect is often discussed in the context of the path integral formulation of quantum mechanics where one compares the wavefunctions passing along two (distinct) paths in a vector potential associated with some magnetic field $\boldsymbol{B}$. Here, the author presents M. V. Berry's interpretation of the Aharonov-Bohm effect as a Berry phase change [1]. This presentation is not only a highly illustrative application of (1), but also avoids issues with single-valuedness of wavefunctions that arise in [2] and [3].

To start, consider particles of mass m and charge q in a magnetic field $\boldsymbol{B}$ generated by a thin long solenoid. For positions $\boldsymbol{R}$ outside the solenoid and enclosing it by a closed path C, the magnetic field is zero but the circulation of $\boldsymbol{A}$ along C is the total magnetic flux:

$$\oint_C \boldsymbol{A}(\boldsymbol{R})\cdot d\boldsymbol{R} = \Phi_B.$$

Let the particles be confined to a box at $\boldsymbol{R}$. The particle Hamiltonian depends on position $\boldsymbol{r}$ and conjugate momentum $\boldsymbol{p}$ as $\mathcal{H} = \mathcal{H}(\boldsymbol{p}, \boldsymbol{r}-\boldsymbol{R})$ in the case when $\boldsymbol{A} = 0$. Let the wavefunctions be $\psi_n(\boldsymbol{r}-\boldsymbol{R})$ with eigenvalues E_n. When $\vec{A} \neq 0$, the Hamiltonian satisfies

$$\mathcal{H}(\boldsymbol{p} - q\boldsymbol{A}(\boldsymbol{R}), \boldsymbol{r}-\boldsymbol{R})\,|n(\boldsymbol{R})\rangle = E_n\,|n(\boldsymbol{R})\rangle$$

since the vector potential does not affect the energies. The solutions for this Hamiltonian,

$$\langle \boldsymbol{r}|n(\boldsymbol{R})\rangle = \exp\left[\frac{iq}{\hbar}\int_{\boldsymbol{R}}^{\boldsymbol{r}} d\boldsymbol{r}'\cdot\boldsymbol{A}(\boldsymbol{r}')\right]\psi_n(\boldsymbol{r}-\boldsymbol{R}),$$

can be obtained by considering the gauge freedom of $\boldsymbol{A}$ and the fact that $\boldsymbol{B} = 0$ for all $\boldsymbol{R}$. With this, we can calculate the total phase change after transporting the box around C. Starting with

$$\begin{aligned} &\langle n(\boldsymbol{R})|\,\nabla_{\boldsymbol{R}}\,|n(\boldsymbol{R})\rangle \\ &= \int d^3\boldsymbol{r}\psi_n^*(\boldsymbol{r}-\boldsymbol{R})\left[\frac{-iq}{\hbar}\psi_n(\boldsymbol{r}-\boldsymbol{R}) + \nabla_{\boldsymbol{R}}\psi_n(\boldsymbol{r}-\boldsymbol{R})\right] \\ &= -\frac{iq\boldsymbol{A}(\boldsymbol{R})}{\hbar}, \end{aligned}$$

we find

$$\gamma_n(C) = \frac{q}{\hbar}\oint_C \boldsymbol{A}(\boldsymbol{R})\cdot d\boldsymbol{R} = \frac{q\Phi_B}{\hbar}.$$

Note that that $\psi_n(C)$ is independent of both n and C, so long as C encloses the solenoid once.

III. ATOM INTERFEROMETRY

In optical interferometry, light waves from a single source travel different paths and interfere constructively or destructively when recombined depending on the relative phase they have accumulated along their paths. The interference pattern allows one to extract information about difference in the path length or refractive index.

Matter-wave interferometry works based on similar principles, relying on the wave-like nature of particles. Following the first[1] observation of the magnetic Aharonov-Bohm effect in the late 1980s using electron matter-waves [4], new developments in atomic, molecular, and optical physics led to interferometry using neutral atoms (an early example is [9]). Atom interferometry are well-suited for precision measurements, gravitational wave sensors, and tests of tests of relativity due to their short de Brogile wavelengths compared to their optical counterpart as well as having nonzero mass, which allows them to interact with gravity [10], [11], [12]. Moreover, atoms possess high controllability thanks to their internal structure and lack electric charge, making them incredible sensors which are immune to undesired environmental influences such as stray electric or magnetic fields [13].

While early atom interferometers such as that developed by [9] used slits and wires to split and reflect atoms, modern iterations manipulate atoms using light forces [14]. These are called light-pulse atom interferometers [15]. In atom interferometers, light and matter invert their roles: when light resonantly interacts with an atom,

[1] [4] is the first undisputed observation of the Aharonov-Bohm effect, where superconductors were used to completely shield electron waves from leakage magnetic fields. Previous observations due to [5], [6] and others in the early 1960s might have suffered from leakage fields, as suggested by [7] and [8].

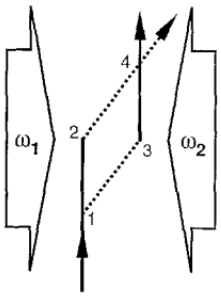

FIG. 1. Lines show the (mean) paths of an atom in an MZ atom interferometer. The solid (dash) lines correspond to the ground (excited) state of the atom. Taken from [15].

Rabi oscillations occur. A $\pi/2$ pulse put an atom in a 50:50 superposition of the ground and excited state and therefore act as a beamsplitter, while a π pulse inverts the population of the ground and excited states, acting as a mirror. To see how atoms are deflected using light, we must take into account the photon momentum. The light pulses correlate the internal states of an atom to its momentum states: an atom in its ground state $|g\rangle$ with momentum $\boldsymbol{p}$ (denoted by $|g,\boldsymbol{p}\rangle$) is coupled to an excited state $|e\rangle$ with momentum $\boldsymbol{p}+\hbar\boldsymbol{k}$ (denoted by $|e,\boldsymbol{p}+\hbar\boldsymbol{k}\rangle$).

In the upcoming subsections, some basic principles of atom interferometry are outlined. Subsections III A and III B describe the most common atom interferometer configurations. Subsections III C and III D present the theory behind stimulated Raman transitions and Bragg diffraction, two powerful mechanisms for splitting and reflecting atoms using laser light.

A. Mach-Zehnder (MZ) atom interferometer

Many atom interferometers have the MZ configuration. In an optical MZ interferometers, a light beam is split by a beamsplitter into two beams which travel different paths and are then redirected towards each other by mirrors and recombined by a beamsplitter, making the beams interfere with each other. The following description of an MZ atom interferometer follows from [15]. In an MZ atom interferometer (see Figure 1), a $\pi/2-\pi-\pi/2$ pulse sequence is used to coherently split, reflect, and recombine an atomic wavepacket. The initial $\pi/2$ puts $|g,\boldsymbol{p}\rangle$ into $|g,\boldsymbol{p}\rangle+|e,\boldsymbol{p}+\hbar\boldsymbol{k}\rangle$, corresponding to two wavepackets. While $|e\rangle$ is stable against spontaneous decay to $|g\rangle$, the two wavepackets drift apart by a distance $\hbar kT/m$ over a duration T. Then, the π pulse inverts the population: $|e,\boldsymbol{p}+\hbar\boldsymbol{k}\rangle \rightarrow |g,\boldsymbol{p}\rangle$ and $|g,\boldsymbol{p}\rangle \rightarrow |e,\boldsymbol{p}+\hbar\boldsymbol{k}\rangle$, and the wavepackets overlap after another interval T. The second $\pi/2$ pulse "recombines" the wavepackets and causes them to interfere.

B. Ramsey-Bordé atom interferometer

Let's not go into this probably... Tell the reader they can read about this stuff at the end of the MZI section, but let's got tangled here. This stuff is actually more complicated than I thought.

C. Stimulated Raman Transition

As is the case in optical interferometry where longer arm lengths increase the instrument's sensitivity, in atom interferometry the larger the wavepacket separation $\hbar kT/m$ the better. However, there is delicate tradeoff between drift time and recoil velocities. Drift times on the order of 1s generally require metastable atomic transitions. While hyperfine transitions easily fulfill this requirement, the recoil velocities are small ($\sim 0.1\mu$m for the Na $F=1,3S_{1/2} \rightarrow F=2,3S_{1/2}$). Metablestable optical transitions have large recoil velocities, but they need ultra-stable lasers to drive.

Stimulated Raman Transitions (SRT) is one of the first techniques developed for obtaining large recoil kicks while simultaneously meeting the metastability criterion. The following treatment of the theory follows from [15].

load theory here!

D. Bragg Diffraction

Bragg diffraction is another tool for generating large momentum transfers for atom interferometry. Due to the (to be described) multi-photon nature of the process, it may be viewed as an improvement over the two-photon stimulated Raman process. The following treatment of Bragg diffraction follows from [16]. Let ω_0 be the transition frequency, $|g\rangle$ the ground state, and $|e\rangle$ the excited state and $\Omega \equiv \vec{d}_{\rm ge}\cdot\vec{E}_0/\hbar$ be the Rabi frequency, where $\vec{d}_{\rm ge}$ is the dipole moment matrix element of the atom. Consider the interaction between the atom and an electric field of the form $\vec{E}=\vec{E}_0(e^{ikz-i\omega_L t}+e^{-ikz+i\omega_L t})/2$. In the near-resonance limit where $\Delta\equiv\omega_L-\omega_0\ll\omega_0$, we may make the rotating wave approximation[2] to obtain

$$\mathcal{H}=\underbrace{\frac{\vec{p}^{\,2}}{2m}+\hbar\omega_0\,|e\rangle\langle e|}_{\equiv\mathcal{H}_0}-\left(\frac{\hbar\Omega}{2}e^{ikz-i\omega_L t}\,|e\rangle\,\langle g|+h.c.\right).$$

For generalized electric fields, $\vec{E}=\sum_j\vec{E}_j\cos(k_j z-(\omega_L-\delta_j)t)$, a generalized rotating

[2] The procedure is standard: Go to the frame rotating at ω_L, eliminate the rapidly rotating term $e^{\pm i(\omega_L+\omega_0)t}$, then transform back to the stationary frame.

wave approximation gives

$$\mathcal{H} \approx \mathcal{H}_0 - \left(\sum_j \frac{\hbar\Omega_j}{2} e^{ik_j z - i(\omega_L - \delta_j)t} \left|e\right\rangle \left\langle g\right| + h.c. \right)$$

where $|\delta_j| \ll \omega_L$ are small detunings from the "main" frequency ω_L and $\Omega_j \equiv \vec{d}_{\rm ge} \cdot \vec{E}_j/\hbar$. Going back to the rotating frame, the Hamiltonian is

$$\begin{aligned}\mathcal{H}^{\rm rot} =& \frac{\vec{p}^2}{2m} - \hbar\Delta \left|e\right\rangle\!\left\langle e\right| \\ & - \left(\sum_j \frac{\hbar\Omega_j}{2} e^{ik_j z + i\delta_i t} \left|e\right\rangle \left\langle g\right| + h.c. \right)\end{aligned}$$

In Bragg diffraction, the electric field is a nearly-standing wave. After the rotating wave approximation,

$$\vec{E} \to \frac{\vec{E}_0}{2} u(z,t) = \frac{\vec{E}_0}{2} \left[e^{-ikz + i\delta t} + e^{ikz - i\delta t} \right] \tag{2}$$

where k is the laser wavevector, 2δ is the detuning between the counter-propagating beams. With this,

$$\mathcal{H}^{\rm rot} = \frac{\vec{p}^2}{2m} - \hbar\Delta \left|e\right\rangle\!\left\langle e\right| - \left(\frac{\hbar\Omega u(z,t)}{2} \left|e\right\rangle \left\langle g\right| + h.c. \right).$$

The solutions to this Hamiltonian have the form

$$\left|\Psi\right\rangle = e(z,t) \left|e\right\rangle + g(z,t) \left|g\right\rangle.$$

Plugging this ansatz into the Schrödinger equation with $\mathcal{H}^{\rm rot}$ we find

$$i\hbar\dot{e}(z,t) = \frac{\vec{p}^2}{2m} e(z,t) - \hbar\Delta e(z,t) - \frac{\hbar\Omega}{2} u g(z,t) \tag{3}$$

$$i\hbar\dot{g}(z,t) = \frac{\vec{p}^2}{2m} g(z,t) - \frac{\hbar\Omega^*}{2} u^* e(z,t). \tag{4}$$

Since $\Delta \gg \Omega$, we may set $\dot{e}(z,t) = 0$. Moreover, $\Delta \gg \omega_r = \hbar k^2/2m$, the recoil frequency, and so $\vec{p}^2/2m \ll \hbar\Delta$ in (3). Solving for $e(z,t)$ and substituting into (4) gives

$$i\dot{g}(z,t) = -\frac{\hbar}{2m}\partial_z^2 g(z,t) + \frac{|\Omega|^2}{4\Delta} u u^* g(z,t). \tag{5}$$

Since the electric field $\sim u(z,t)$ is periodic, we may choose the following ansatz for $g(z,t)$:

$$g(z,t) = \sum_{-\infty}^{\infty} g_n(t) e^{i2nkz} e^{-i(2n)^2\omega_r t}. \tag{6}$$

Inserting this ansatz into (5) and simplifying[3] gives

$$\begin{aligned}i\dot{g}_n =& \frac{\bar{\Omega}}{2} g_{n+1} e^{i2\delta t} e^{-i4(2n+1)\omega_r t} \\ & + \frac{\bar{\Omega}}{2} g_{n-1} e^{-i2\delta t} e^{i4(2n-1)\omega_r t}.\end{aligned} \tag{7}$$

[3] The reader may refer to [16] for details regarding this step.

where $\bar{\Omega} = |\Omega|^2/2\Delta$ is the two-photon Rabi frequency. This is an infinite set of coupled differential equations where the plane wave momentum states of the atom are coupled only by integer multiples of the photon wavevector k. An atom starting in g_{n_I} with momentum $2n_I\hbar k$ can only be transferred to g_{n_F}'s with momentum $2n_F\hbar k$. The Bragg resonance condition for this process is $\delta = 2(n_F + n_I)\omega_r$.

Consider a system where an atom initially in a pure momentum state $g_{n_I} = 1$ is resonantly transferred to a state g_{n_F} via $\delta = 2(n_I + n_F)\omega_r$. For sufficiently long interaction times, terms proportional to $e^{i4(\pm 2j \pm 1)}$ for $|j| \gg n$ oscillate rapidly and may be taken to be zero. We can then choose cutoffs $n_+ > \max(n_I, n_F)$ and $-n_- < \min(n_I, n_F)$ so that (7) is reduced to a finite system:

$$\begin{aligned}i\dot{g}_{n_+ + 1} &= 0 \\ &\vdots \\ i\dot{g}_n &= \frac{\bar{\Omega}}{2} g_{n+1} e^{i2\delta t} e^{-i4(2n+1)\omega_r t} \\ &\quad + \frac{\bar{\Omega}}{2} g_{n-1} e^{-i2\delta t} e^{i4(2n-1)\omega_r t} \\ &\vdots \\ i\dot{g}_{-n_- - 1} &= 0,\end{aligned}$$

which can be solved numerically. Figure 2, taken from [16], shows the relevant momentum states of an atom and laser fields for Bragg diffraction, transferring atoms from $|g, 0\hbar k\rangle$ to $|g, 6\hbar k\rangle$. The detuning of the undesired $2m$-photon process $|g, 0, \hbar k\rangle \to |g, 2m\hbar k\rangle$ is $2m\delta - 4m^2\omega_r$. So the undesired intermediate states (solid blue, $m \neq n$) to remain unpopulated, δ_m for $m \neq n$ must be much greater than $\bar{\Omega}$. In practice, efficient transfers are determined by a number of factors including the time-dependence of the two-photon Rabi frequency, pulse width, shape, and the momentum spread of the atoms. A detailed discussion of these parameters in [16] is beyond the scope of this paper, but it is important to mention the last point regarding moving atoms. Our discussion so far has been confined to the case where the atoms are at rest relative to the standing wave ($\delta = 0$) caused by the Bragg beams. When $g_0(t)$ has some velocity Δv, then the ansatz (6) is modified, and the system of coupled differential equations becomes

$$\begin{aligned}i\dot{g}_n =& \frac{\bar{\Omega}}{2} \left[g_{n+1} e^{i2(\delta - 2\omega_r \Delta v/v_r)t} e^{-i4(2n+1)\omega_r t} \right] \\ & + \frac{\bar{\Omega}}{2} g_{n-1} e^{-i2(\delta - 2\omega_r \Delta v/v_r)t} e^{i4(2n-1)\omega_r t},\end{aligned}$$

where $v_r = \hbar k/m$ is the recoil velocity. In this case we see that atoms with net velocity Δv are out of resonance with the Bragg condition $\delta = 2(n_F + n_I)\omega_r$ by $2\omega_r\Delta/v_r$, but still only couple to higher or lower momentum states by multiples of $2\hbar k$. This is crucial since in practice atoms for an interferometer always have a finite velocity distribution.

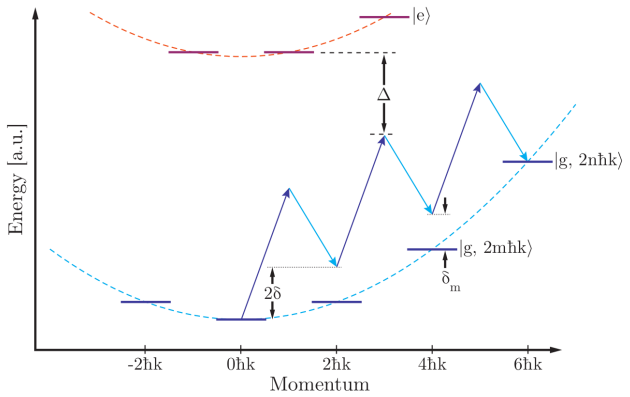

FIG. 2. Relevant momentum states of an atom and laser fields for Bragg diffraction. 2δ is the detuning between counter-propagating Bragg beams. Δ is the single-photon detuning of the lasers from $|e\rangle$. δ_m is the multi-photon detuning to an arbitrary intermediate ground state $|g, m\hbar k\rangle$. Figure taken from [16].

IV. OBSERVATION OF A GRAVITATIONAL AHARONOV-BOHM EFFECT

Talk about HM's proposal 10 years ago and talk about the observation today. [17], [18].

V. CONCLUSIONS

The subject is incredibly rich... can't possibly by covered in a few pages. There are deep theory calculating phase shifts which is beyond the scope here. There are also applications, techniques, etc that I have not mentioned.

Probably list a bunch of places where the reader can read stuff.

ACKNOWLEDGMENTS

The author would like to thank Professor Martin Zwierlein for the exciting AMO physics lectures. 8.421: AMO I is the first *official* course in atomic physics for the author. The author very much looks forward to continuing his studies in 8.422: AMO II.

[1] M. V. Berry, Proceedings of the Royal Society of London. A. Mathematical and Physical Sciences **392**, 45 (1984).
[2] Y. Aharonov and D. Bohm, Physical Review **115**, 485 (1959).
[3] W. Ehrenberg and R. E. Siday, Proceedings of the Physical Society. Section B **62**, 8 (1949).
[4] A. Tonomura, N. Osakabe, T. Matsuda, T. Kawasaki, J. Endo, S. Yano, and H. Yamada, Physical review letters **56**, 792 (1986).
[5] R. Chambers, Physical Review Letters **5**, 3 (1960).
[6] H. Fowler, L. Marton, J. A. Simpson, and J. Suddeth, Journal of Applied Physics **32**, 1153 (1961).
[7] P. Bocchieri and A. Loinger, Il Nuovo Cimento A (1965-1970) **47**, 475 (1978).
[8] S. Roy, Physical Review Letters **44**, 111 (1980).
[9] D. W. Keith, C. R. Ekstrom, Q. A. Turchette, and D. E. Pritchard, Physical review letters **66**, 2693 (1991).
[10] H. Mueller, Atom Interferometry, Proceedings of the International School of Physics "Enrico Fermi **188**, 339 (2014).
[11] S. Dimopoulos, P. W. Graham, J. M. Hogan, M. A. Kasevich, and S. Rajendran, Physics Letters B **678**, 37 (2009).
[12] B. Stray, A. Lamb, A. Kaushik, J. Vovrosh, A. Rodgers, J. Winch, F. Hayati, D. Boddice, A. Stabrawa, A. Niggebaum, *et al.*, Nature **602**, 590 (2022).
[13] K. Bongs, M. Holynski, J. Vovrosh, P. Bouyer, G. Condon, E. Rasel, C. Schubert, W. P. Schleich, and A. Roura, Nature Reviews Physics **1**, 731 (2019).
[14] E. M. Rasel, M. K. Oberthaler, H. Batelaan, J. Schmiedmayer, and A. Zeilinger, Physical Review Letters **75**, 2633 (1995).
[15] M. Kasevich and S. Chu, Applied Physics B **54**, 321 (1992).
[16] B. V. Estey, *Precision Measurement in Atom Interferometry Using Bragg Diffraction*, Ph.D. thesis, UC Berkeley (2016).
[17] M. A. Hohensee, B. Estey, P. Hamilton, A. Zeilinger, and H. Müller, Physical Review Letters **108**, 230404 (2012).
[18] C. Overstreet, P. Asenbaum, J. Curti, M. Kim, and M. A. Kasevich, Science **375**, 226 (2022).